Available online at www.sciencedirect.com
SCIENCE DIRECT
Journal of Colloid and Interface Science 292 (2005) 255–264
JOURNAL OF Colloid and Interface Science
www.elsevier.com/locate/jcis

Giant vesicles of a single-tailed chiral cationic surfactant, (1R,2S)-(–)-*N*-dodecyl-*N*-methylephedrinium bromide, in water

Sumita Roy, Dibyendu Khatua, Joykrishna Dey *

Department of Chemistry, Indian Institute of Technology, Kharagpur 721 302, India

Received 19 March 2005; accepted 18 May 2005

Available online 15 July 2005

Abstract

Self-assembly properties of a single-tailed chiral cationic surfactant, (1R,2S)-(–)-*N*-dodecyl-*N*-methylephedrinium bromide (DMEB), have been studied in water. The molecular self-assemblies of the amphiphile have been characterized by surface tension, fluorescence probes, light scattering, and microscopic techniques. The results have been compared with those of dodecyltrimethylammonium bromide (DTAB) surfactant. The critical aggregation concentration of DMEB was found to be much less than that of DTAB. Surface tension and fluorescence probe studies have suggested formation of micellar structures at low temperature (<28 °C) and spontaneous formation of giant vesicles in water above 28 °C. The mean size of the aggregates has been measured by a dynamic light scattering method. The micropolarity and microviscosity of the self-assemblies were determined by fluorescence probe technique. The ^{1}H NMR and FTIR spectra were recorded to elucidate the role of the hydrophobic head group towards the formation of bilayer structures. The phase transition temperatures of the vesicular aggregates were determined by measurement of fluorescence anisotropy at various temperatures.

Keywords: Vesicle; Surface tension; Fluorescence; Microviscosity; Light scattering; Microscopy

1. Introduction

There have been many reports on vesicle formation from natural amphiphiles (mainly phospholipids) and synthetic surfactants in the past three decades [1,2]. Vesicles formed by synthetic surfactants, in particular, have attracted attention because of their potential uses as agents for encapsulation and eventual release of drugs, flavors, and fragrances, and also as microreactors for the synthesis of monodispersed nanometer-sized semiconductor particles [3–6]. Giant vesicles can also serve as models for biological membranes. The hydrophobic groups of the amphiphiles that have been used to form vesicles include two kinds of structures: double-chained and single-chained. Synthetic amphiphiles with different chemical structures and compositions of head groups and hydrocarbon tail(s) that can self-organize into vesicles in dilute aqueous solutions have been discussed in the recent literature [7–13]. Single-tailed cationic surfactants having azo linkages, unsaturation, or biphenyl moieties in the hydrocarbon chain have been found to form vesicles [14–16]. On the other hand, bola amphiphiles have been also reported to form bilayer vesicles [17–20]. Spontaneous vesicle formation from mixed single-chain anionic and cationic surfactants (catanionic mixtures) has been reported in the literature [21–24].

In this work, we report that giant vesicles can be spontaneously formed by self-assembly of a single-tailed cationic surfactant (1R,2S)-(–)-*N*-dodecyl-*N*-methylephedrinium bromide, DMEB (see Scheme 1 for structure). DMEB is used as a phase-transfer catalyst for asymmetric synthesis [25]. Enantiomeric separation of drug molecules by micellar electrokinetic chromatography has also demonstrated the chiral recognition properties of the surfactant in solution [26]. In order to explain the chiral recognition properties of DMEB, it is necessary to understand the aggregation behavior in solution. The present study is a part of our interest

* Corresponding author. Fax: +91 3222 255303.
E-mail address: joydey@chem.iitkgp.ernet.in (J. Dey).

0021-9797/$ – see front matter
doi:10.1016/j.jcis.2005.05.054

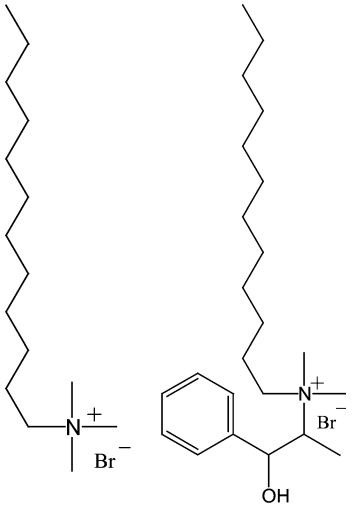

Scheme 1. Molecular structures of DTAB and DMEB.

in microstructures formed by optically active surfactants. Recently, Oremusová et al. [27] have measured the physicochemical properties of the surfactant in water. These authors have determined the critical aggregation concentration of DMEB by various methods. From the measured thermodynamic parameters ($\Delta_m G^0$, $\Delta_m H^0$, and $\Delta_m S^0$) they concluded that London dispersion interaction, not hydrophobic interaction, is the major driving force for the micellization of DMEB molecules. The amphiphile has a chemical structure very similar to that of dodecyltrimethylammonium bromide, DTAB (Scheme 1). DMEB is derived from DTAB by replacement of one of the methyl groups of the surfactant head by a phenylalkyl group that carries two stereogenic centers and an –OH group. The –OH group can in principle form intermolecular hydrogen bonds. Therefore, we are interested to investigate how the structural features bear on the microstructures of the molecular self-assemblies of the amphiphile in water. The objectives of the present study are (i) to study the aggregation properties in water, (ii) to investigate the microenvironment of the self-assemblies, (iii) to measure the mean size of the aggregates, and (iv) to examine the microstructure in order to determine the shape as well as size of the aggregates. The results will be compared with those of DTAB surfactant. The ^{1}H NMR and FTIR spectra will be used to shed light on the role of the phenyl moiety in the formation of self-assemblies.

2. Experimental section

2.1. Materials

Pyrene (99%), 1, 6-diphenylhexatriene, DPH (99%), 1-anilinonaphthalene, AN (98%), and DMEB (99%) were purchased from Aldrich. The purity of DMEB, which melted sharply at 82 °C, was confirmed by ^{1}H NMR spectrum (see Fig. 1 under Supplementary material). Therefore, DMEB was used without further purification. But pyrene, AN, and DPH were recrystallized several times from acetone–ethanol mixture. Purity of the probes was tested by the fluorescence emission and excitation spectra. Cetylpyridinium chloride was from SRL. It was purified by recrystallization from ethanol. All solutions were prepared using Milli-Q water (18.2 Ω).

2.2. Methods

2.2.1. General instrumentation

The UV–visible spectra were recorded on a Shimadzu (Model 1601) spectrophotometer. The FTIR spectra were measured with a Thermo Nicolet Nexus 870 spectrometer. The ^{1}H NMR spectra were measured with a Bruker 250 MHz instrument. The density of a solution was measured by weighing method using a dilatometer. All measurements were done at room temperature (∼30 °C) unless otherwise mentioned. Conductivity was measured with a Thermo Orion (Model 150A+) conductivity meter that uses a four-electrode cell of cell constant equal to 0.467.

2.2.2. Surface tension measurements

The surface tension measurements were performed with a torsion balance (S.D. Hurdson & Co., Kolkata) using the Du Nuoy ring detachment method. Temperature-controlled (±0.1 °C) measurements were carried out by use of a Thermo-Neslab RTE 7 circulating bath. A stock solution of DMEB was made in Milli-Q water. Aliquot of this solution was transferred to a beaker containing known volume of water. The solution was gently stirred magnetically and allowed to stand for about 5 min at room temperature and then the surface tension was measured. For each measurement at least three readings were taken and the mean γ value was recorded. Before each experiment the instrument was calibrated and checked by measuring the surface tension of distilled water.

2.2.3. Steady-state fluorescence measurements

The steady-state fluorescence spectra were recorded with a SPEX Fluorolog Model FL3-11 spectrofluorometer using a 1-cm^2 quartz cuvette. Saturated aqueous solutions of pyrene and AN were used for sample preparation. The samples containing pyrene and AN were excited at 335 and 350 nm, respectively. The emission spectra were recorded between 350 and 550 nm using both excitation and emission slits with bandpass equal to 1.0 nm. Each spectrum was blank subtracted and corrected for lamp intensity variation during the experiment.

Steady-state fluorescence anisotropy (r) was measured on a Perkin–Elmer LS-55 luminescence spectrometer equipped with a thermostated cell holder and filter polarizers that used the L-format configuration. The temperature was controlled within ±0.1 °C by a Thermo Neslab (Model RTE 7) water-circulating bath. Since DPH is insoluble in water, a 1.0 mM

stock solution of the probe in 20% (v/v) methanol–water mixture was prepared. The final concentration of the probe was adjusted to 2.0 μM by addition of an appropriate amount of the stock solution. The sample was excited at 350 nm and the emission intensity was followed at 450 nm using excitation and emission slits with bandpass of 2.5 and 5 nm, respectively. A 430-nm cutoff filter was placed in the emission beam to reduce effects due to scattered radiation. The r-value was calculated employing the equation

$$r = (I_{VV} - G I_{VH})/(I_{VV} + 2G I_{VH}), \quad (1)$$

where I_{VV} and I_{VH} are the fluorescence intensities polarized parallel and perpendicular to the excitation light, and G is the instrumental correction factor ($G = I_{VV}/I_{VH}$).

2.2.4. Time-resolved fluorescence measurements

The time-resolved fluorescence intensity decay was measured with a picosecond time-correlated single-photon-counting (TCSPC) spectrofluorometer. A mode-locked Ti: Sapphire laser (Spectra Physics, Tsunami 3950M 3S) pumped by a diode-pumped CW visible laser (Spectra Physics, Milenia SN 1638) was used as a light source. The frequency-doubled output laser ($\lambda = 370$ nm) obtained by a flexible harmonic generator (Spectra Physics, GWU 23 PS) was used for sample excitation. The decay kinetics was recorded at the emission wavelength of 450 nm. The emission was detected by magic angle (54.7°) polarization using a Hamamatsu MCP photomultiplier tube (2809 U). The instrument response function of the system was ∼49 ps. The decay was analyzed by IBH DAS-6 decay analysis software. The goodness of the data fit was judged by the χ^2-value (in the range 1–1.2) and by the randomness of residual function.

2.2.5. Light scattering measurements

The dynamic light scattering (DLS) measurements were performed with a Photal DLS-7000 (Otsuka Electronics Co. Ltd., Osaka, Japan) optical system equipped with an Ar^+ ion laser (75 mW) operated at 16 mW at $\lambda_0 = 488$ nm, a digital correlator, and a computer-controlled and stepping-motor-driven variable angle detection system. An 8 mM solution of the amphiphile was prepared in Milli-Q water. The solution was filtered directly into the scattering cell through a Millipore Millex syringe filter (Triton free, 0.22 μm). Before measurement, the scattering cell was rinsed several times with the filtered solution. The DLS measurements started 5–10 min after the sample solutions were placed in the DLS optical system to allow the sample to equilibrate at the bath temperature. The scattering intensity was normally measured at $\theta = 90^o$ to the incident beam. Some measurements however, were performed at low angles in the range of 20°–60°. Each experiment was repeated two or three times. The data were analyzed using the second-order cumulant method.

2.2.6. Microscopy

The microscopic measurements were performed using an 8 mM clear solution of DMEB. The specimen was made by placing a drop of the aqueous solution on a 200 mesh size carbon-coated copper grid, waiting for a minute, and then blotting off the excess liquid with filter paper. After half an hour of air-drying the specimen was negatively stained with a freshly prepared 2% aqueous solution of phosphotungstic acid, the pH of which was adjusted to solution pH by adding KOH solution. The stained specimen was dried in a desicator and was examined on a Phillips CM 12 electron microscope operating at 120 kV. For optical micrographs, a drop of the filtered solution was placed on a thoroughly cleaned glass plate and covered with a coverslip. The light micrographs were obtained from a Leica-DMRXP microscope. The images taken by a video camera were analyzed by Leica Qwin software.

3. Results and discussion

3.1. Solubility studies

The DMEB is poorly soluble in water below room temperature. Because of poor solubility, most of the studies described below, unless otherwise mentioned, were carried out at room temperature (∼30 °C). The saturated aqueous solutions of DMEB at all temperatures studied were transparent. A suspension of DMEB (10.3 g L^{-1}) was initially heated to make a clear solution. It was then allowed to equilibrate at 10 °C for 24 h. The solubility was examined by measuring conductivity of the suspension at various temperatures. The plot in Fig. 1 shows the variation of conductivity as a function of temperature. The plot shows that conductivity increases sharply above 25 °C. This means rise of solubility of the surfactant with increase in temperature. The temperature (28 °C) corresponding to the inflection point of the curve is often referred to as the Krafft temperature, T_K. This, however, should not be confused with the Krafft point (T_P) that

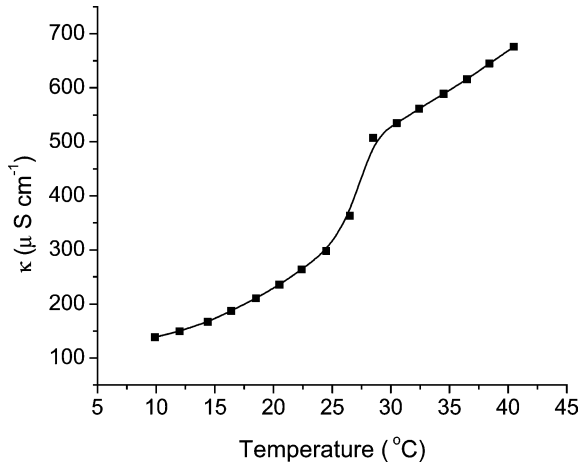

Fig. 1. Plot of conductivity (κ) as a function of temperature.

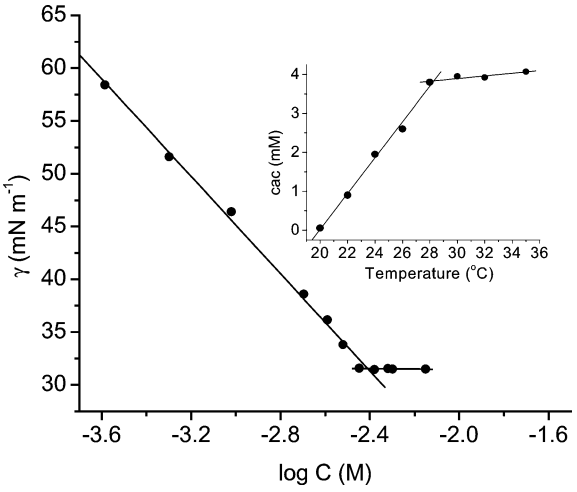

Fig. 2. Plot of surface tension (γ) vs $\log C$ of DMEB at 30 °C. Inset: plot of cac vs temperature.

defines the temperature at which the solubility of the surfactant becomes equal to its critical micelle concentration [28]. This means that micellar aggregates do not exist below T_P. On the other hand, micelles may form below T_K. This is confirmed by fluorescence probe studies described below.

3.2. Critical aggregation concentration (cac)

3.2.1. Surface tension method

The surface tension (γ) measurements were used to determine the cac of DMEB. Among the various methods available for the determination of the cac the surface tension (ST) is known to be the most accurate method. The typical plot of γ versus $\log C$ at 30 °C is shown in Fig. 2. The γ value decreases linearly with $\log C$ and show a characteristic break and remain constant thereafter. The break point corresponds to the cac value. No minimum around the cac can be observed in the plots. This confirms the purity of the surfactant. The surface properties of DMEB are listed in Table 1. For comparison purposes, we have also included in Table 1 the corresponding data for DTAB that are already reported in the literature [29]. The cac value (4.0 mM) of DMEB is close to the value (4.08, 4.12 mM) reported by others [27]. The surface pressure, π_{cac} ($\pi_{cac} = \gamma_{water} - \gamma_{solution}$) values corresponding to cac suggest that both DMEB and DTAB are equally good surface-active agents. Although the hydrocarbon chain lengths of DMEB and DTAB are equal, the cac value of the former is much less than that of DTAB. This implies that the formation of micelles is more favorable in the case of DMEB than in DTAB surfactant. This is perhaps due to the π–π and intermolecular hydrogen-bonding interactions between phenylalkyl moieties of two neighboring surfactant molecules. The low cac value is also indicative of the formation of larger aggregates compared to that of DTAB, which is known to form small micelles with a mean aggregation number equal to 48 [29]. The cac values of DMEB at different temperatures above and below room temperature

Table 1
Critical aggregation concentration (cac), surface pressure (π_{cac}) at cac, maximum surface excess concentration (Γ_{max}), minimum surface area per headgroup (A_0), hydrodynamic radius (R_h), aggregation number (N_{agg}) micropolarity (I_1/I_3), microviscosity (η_m), and phase transition temperatures (T_c, T_m) of DMEB and DTAB at 303 K

Properties	DMEB	DTAB[a]
cac (mM)	4.0, 3.9[b]	14.7
π_{cac} (mN m^{-1})	39.0	39.0
$\Gamma_{max} \times 10^{-6}$ (mol m^{-2})	1.99	1.40
A_0 (nm^2)	0.84 ± 0.05	1.18
R_h (nm)	165, 1100	1.39
N_{agg}	81.5×10^4	48.0
I_1/I_3	1.21	1.42
η_m (mPa s)	30.75	13.23[c]
T_c (K)	301.0	–
T_m (K)	316.5	–

[a] Values are taken from Ref. [29].
[b] Obtained from fluorescence measurements using pyrene as probe.
[c] This work.

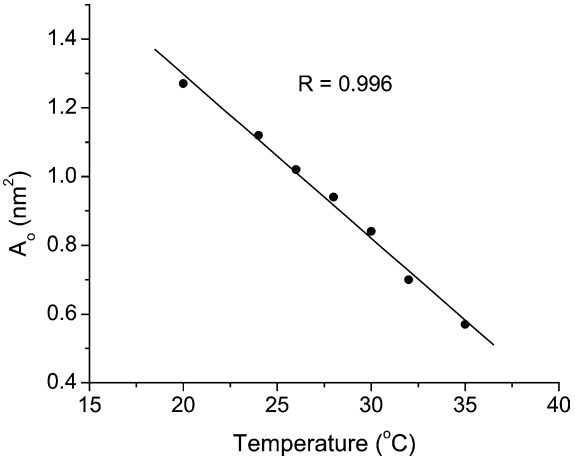

Fig. 3. Variation of surface area/headgroup (A_0) with temperature.

were also determined by the ST method. The plot of the variation of cac with temperature is shown as an inset of Fig. 2. It is interesting to note that the plot exhibits a breakpoint corresponding to a temperature of 28 °C, which is equal to the T_K value. This suggests that there must be some connection between the variations of conductivity (i.e., solubility) and cac with temperature. The plot also suggests that DMEB do form aggregates below T_K. The minimum surface area per surfactant headgroup, A_0, at the air/water interface was estimated from the slope of the linear part of the ST plot using the Gibbs adsorption equation [30,31]. The room temperature value of A_0 for DMEB (Table 1) is less than 1.0 nm^2 and is also less than that of the DTAB surfactant. Normally, A_0 is expected to increase upon increase of temperature as aggregates start to break down. In contrast, the A_0 value decreased continuously with the increase in temperature (Fig. 3) in the range (20–35 °C) studied. This suggests stronger interactions between surfactant molecules. The $A_0 < 1.0$ nm^2 is indicative of the formation of bilayer aggregates [32]. Since the A_0 value for DMEB is greater than 1.0 nm^2 below 28 °C,

it can be assumed that DMEB forms small micellar aggregates at temperatures below T_K. Above T_K the micelles transform into bilayer structures. Therefore, T_K can be taken as the micelle-to-bilayer phase transition temperature. The same is also true with the breakpoint in the cac versus temperature plot in Fig. 2. Thus the cac values above T_K can be referred to as critical vesicle concentrations (cvc). Further evidence in favor of the formation of vesicle structures is discussed below.

3.2.2. *Fluorescence probe method*

In order to demonstrate the formation of aggregates by DMEB molecules below T_K we have measured fluorescence spectra of AN probe at 10 °C in the presence and absence of the surfactant. The fluorescence spectrum of AN (inset of Fig. 4) in 3.5 mM DMEB solution is blue-shifted compared to that in water, accompanied by a large increase in intensity. This suggests that the probe molecules are solubilized within a hydrophobic environment, which means aggregate formation by DMEB molecules at 10 °C. This also indicates that the Krafft point of the DMEB surfactant is less than 10 °C.

The polarity of the hydrophobic domains of the aggregates can be estimated by a fluorescence probe technique. Pyrene is a well-known fluorescence probe for the micropolarity studies of its solubilization site in micellar interiors [33–37]. The intensity ratio I_1/I_3 of the third and the first vibronic peaks of the pyrene fluorescence spectrum is very sensitive to solvent polarity [38] and therefore has been widely used as a measure of the polarity of the microenvironment of the probe [33–37]. Normally, low values of I_1/I_3 indicate a nonpolar environment whereas high values indicates polar environment. The apparent micropolarity of the aggregates was therefore estimated by measuring the I_1/I_3 ratio at various surfactant concentrations. The data are plotted in Fig. 4, which shows a sigmoid decrease of the I_1/I_3 ratio with the increase of DMEB concentration. The concentration (3.9 mM) corresponding to the inflection point can be taken as the cac. This value is very close to the one obtained from surface tension studies. The low value of the I_1/I_3 ratio compared to that in water (1.81) above the cac indicates that the probe molecules are solubilized in a nonpolar environment of spherical aggregates [38]. The data in Table 1 suggest that the microenvironment of the probe in DMEB is more nonpolar than that in DTAB micelles [29]. This suggests enhanced ordering (compared to that in DTAB micelles) at the aggregate–water interface of DMEB aggregates that reduces the degree of water penetration in the hydrocarbon layer, in accordance with the reduction observed in micropolarity sensed by the probe molecules. The enhanced ordering at the interface may result from the insertion of the phenyl moiety between two hydrocarbon chains, which reduces ionic repulsion between the headgroups of DMEB molecules, which means a tighter packing of the hydrocarbon chains in the self-assembly.

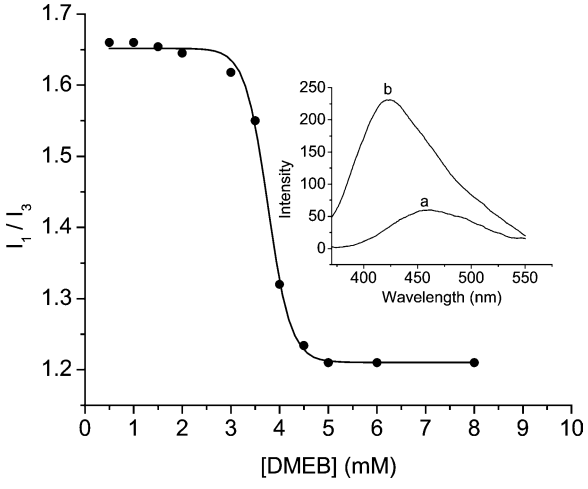

Fig. 4. Plot of I_1/I_3 versus DMEB concentration. Inset: fluorescence spectra of AN in (a) water, (b) 3.5 mM DMEB at 10 °C.

3.3. *Microviscosity*

The tighter packing of the hydrocarbon chains, as discussed in the preceding section, should be manifested by the microviscosity value of the self-assembly. The fluorescence anisotropy (r) measurement provides useful insights into the physical properties of lipid bilayers. DPH is a well-known membrane fluidity probe and has been used for studying many lipid bilayer membranes [39–41]. Therefore the steady-state fluorescence anisotropy of DPH was measured in 8 mM DMEB solution at room temperature. The r-value was found to be 0.115, which is greater than that of DTAB micelles (0.045). The relatively higher value of r at room temperature suggests a more ordered environment around the DPH probe in the self-assembly of DMEB. The r-value is also higher than lecithin liposomes ($r \sim 0.098$) but less than that of sphingomyelin liposomes ($r \sim 0.247$) [41]. This may suggest that the self-assemblies of DMEB formed at or above room temperature have bilayer vesicle structures similar to those of liposomes. On the other hand, below room temperature DMEB, like DTAB, forms micellar aggregates.

In order to compare the microstructure of the self-assemblies of DMEB with those of DTAB micelles, the microviscosity value was determined for both amphiphiles. The relationship between fluorescence anisotropy, r, and microviscosity, η_m, is given by the Perrin–Stokes–Einstein–Debye equation [42],

$$\eta_m = k_B T \tau_f / \left[v_m (r_0/r - 1) \right], \tag{2}$$

where k_B is the Boltzmann constant, T is the absolute temperature, τ_f is the fluorescence lifetime of DPH in micellar environment, v_m is the effective molecular volume of the DPH probe, and r_0 (=0.362) [43,44] is the limiting value of fluorescence anisotropy in a medium of infinite viscosity. The v_m value (313 Å^3) of DPH was estimated by Edward's atomic increment method [45] using experimental molecular volume of *trans*-stilbene (257 Å^3) [45]. The fluorescence lifetime of DPH in the presence of 8 mM DMEB was

found to be 4.94 ns. The fluorescence lifetime (6.97 ns) of DPH in DTAB micelles was taken from the literature [46]. The anisotropy value of DTAB micelles was measured to be 0.045 at 30 °C. The values of η_m calculated by the use of Eq. (2) are listed in Table 1. The η_m value of DTAB micelles is slightly less than that reported for CTAB micelles [47]. This is consistent with the shorter chain length of DTAB compared to CTAB surfactant. However, even though DMEB has same chain length as that of DTAB, the η_m value of the former is almost three times higher than that of the latter micelles. This suggests that the hydrocarbon chains in the bilayer self-assemblies of DMEB surfactant are more tightly packed (i.e., less fluid) than those in DTAB micelles. The magnitude of the microviscosity sensed by the DPH probe solubilized in the self-assemblies of DMEB is comparable to many liposome systems [39,40]. Therefore, it may be concluded that the amphiphile forms liposome-like bilayer membrane structures in aqueous solutions. However, it should be noted that the fluorescence lifetime of DPH in DMEB vesicles is less than that in DTAB micelles. This indicates that the probe molecule is solubilized at the membrane–water interface of DMEB. On the other hand, it is solubilized in the core of DTAB micelle. This is perhaps due to the steric hindrance caused by the phenyl ring at the membrane interface. In other words, the phenyl moiety is oriented toward the hydrophobic region of the vesicle bilayer. The estimated η_m value of DMEB, therefore, reflects the fluidity of the interfacial region of the hydrophobic membrane even though it is higher than that of DTAB micelles.

3.4. Aggregation number

Micellar aggregates have usually very small aggregation numbers compared to that of bilayer vesicles. In order to confirm that DMEB forms micellar structures below room temperature, we have determined the mean micellar aggregation number (N_{agg}) of DMEB at 25 °C. Many authors have successively used the quenching of pyrene fluorescence by a suitable quencher, Q, such as cetylpyridinium chloride (CPC) to determine N_{agg} of micelles using the equation [48,49]

$$\ln(I_0/I) = N_{agg}[Q]/\big([surf] - cac\big), \tag{3}$$

where I_0 and I are the fluorescence intensities in the absence and presence of quencher. In the present study, an 8 mM DMEB solution was used for the measurement. In Fig. 5, $\ln(I_0/I)$ is plotted against CPC concentration. The N_{agg} value of DMEB (85 ± 5) thus obtained from the slope and cac values is almost twice as large as that of DTAB (48) micelles [29]. This is consistent with the low cac and A_0 values of DMEB compared to that of DTAB surfactant. Although the average aggregation number of DMEB is higher than that of DTAB micelles, it does not fit to vesicle structures because the size of the latter is much larger than normal spherical micelles.

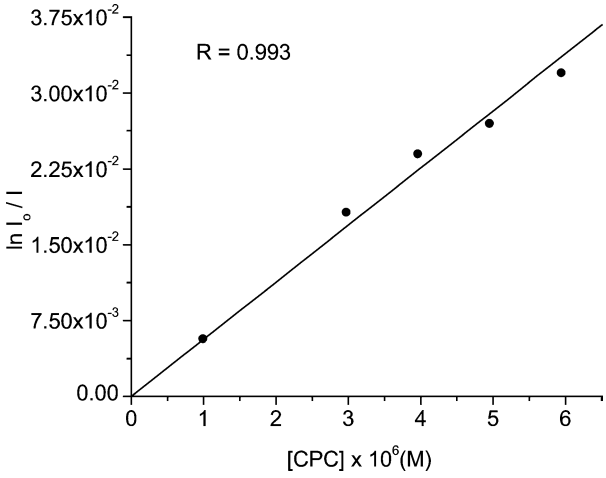

Fig. 5. Plot of $\ln(I_0/I)$ versus CPC concentration.

Wettig et al. [50] developed a calibration curve for the determination of molecular weight (M_W) of micelles from the experimentally determined R_h values and molecular weights calculated from aggregation numbers of n-alkyltrimethylammonium bromide surfactants determined using the fluorescence quenching method. The equation can be written as

$$M_W = -9.855(R_h)^2 + 50.79(R_h) - 30.04, \tag{4}$$

where the molecular weight is in kilodaltons (kDa) and R_h is in nanometers (nm). Since the molecular weight of the DMEB molecule and N_{agg} are respectively 428.51 and 85.0, the molecular weight of the DMEB micelles is 36.42 kDa. Thus, the R_h value of the DMEB micelle obtained from Eq. (4) is 2.57 nm. This is approximately twice the size of DTAB micelles (1.39 nm) [39] and is consistent with its N_{agg} value. However, the size is too small to fit to a vesicle structure. Thus it can be concluded that DMEB forms micellar aggregates at temperatures below T_K. The A_0 (0.98 nm^2) calculated from the R_h and N_{agg} values by the use of the equation [51]

$$A_0 = 4\pi R_h^2/N_{agg} \tag{5}$$

is in good agreement with the value (1.03) obtained by ST measurement. This confirms the accuracy of the N_{agg} value.

3.5. Dynamic light scattering

The dynamic light scattering (DLS) technique is normally used for direct measurement of the hydrodynamic radius, R_h, of colloidal particles. To obtain the mean size of the aggregates we have performed DLS studies to measure the R_h of the aggregates in 8 mM DMEB solution at room temperature (~30 °C). The apparent diffusion coefficient thus obtained, D, is $\sim 10^{-12}$ m^2 s^{-1}, which is much less than that of normal spherical micelles ($D \sim 10^{-10}$ m^2 s^{-1}) [52]. Assuming spherical particles, the R_h value was calculated from the Stokes–Einstein equation,

$$R_h = k_B T/(6\pi\eta D), \tag{6}$$

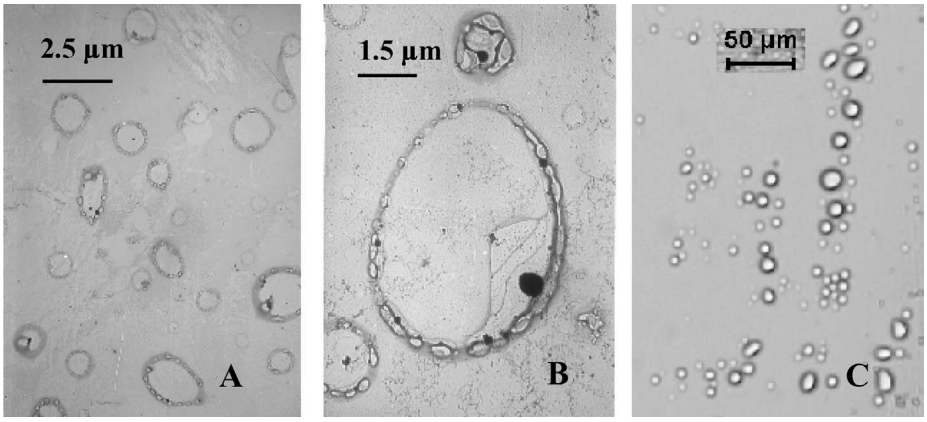

Fig. 6. Negatively stained transmission electron micrographs (A, B), and optical micrograph (C) of 8 mM DMEB in water at 30 °C.

where k_B is the Boltzmann constant, η is the viscosity of the solvent, and D is the apparent translational diffusion coefficient of the aggregates. Thus the R_h value at this temperature was found to be 165 nm, which is too large to fit a micellar aggregate. The only possible spherical aggregates of DMEB that can have sizes as large as 165 nm are large unilamellar or multilamellar vesicles. However, the size of the aggregates increased upon aging. After 5 h the R_h was found to be 1.1 µm. We were unable to measure the hydrodynamic radius directly at 25 °C with our instrument. This might be due to the presence of small ($R_h < 3$ nm) micellar aggregates at low temperatures, as discussed earlier. Indeed, as discussed above, the N_{agg} value at 25 °C has suggested small micelles of R_h equal to 2.57 nm. From the measured R_h and A_0 values we have calculated the N_{agg} value (Table 1) of the vesicles (assuming unilamellar) employing the relationship [53]

$$N_{agg} = 8\pi R_h^2 / A_0. \quad (7)$$

As expected, the N_{agg} value of the vesicles at room temperature is much larger than that of the micellar aggregates formed by the surfactant at 25 °C. Also, the N_{agg} value is much larger than that of DTAB micelles (48.0).

3.6. Microscopic studies

In order to visualize the shape and nature of the self-assemblies of DMEB, we have investigated the microstructures by transmission electron microscopy (TEM). The specimens were prepared using 8 mM aqueous solution at 30 °C. The TEM pictures in Figs. 6A and 6B clearly display closed spherical as well as elliptical vesicles with a broad size (outer diameter) distribution, but most of them are in the range of 0.2–6 µm. This is consistent with the value obtained from DLS measurements. A close examination of the contour curves of the spheres gives a thickness of the vesicle shell of 30–70 nm. This is thicker than that of natural liposomes (3–4 nm) [54]. The large wall thickness suggests that the small as well as the large spheroidal self-assemblies are a multilamellar vesicle. As can be observed in picture B, the giant vesicles are formed through the fusion of small vesicles. Since the size of the vesicles is large, we also measured the optical micrograph of the aqueous solution of DMEB. The micrograph is shown in Fig. 6C. The microstructures clearly indicate the presence of spheroidal vesicles having sizes in the range of 4–20 µm. Similar structures were also observed under the microscope after 15 days, thus confirming the stability of the vesicles. The aggregate sizes revealed by optical microscopy are slightly larger than those obtained from TEM measurement. This might be due to the artifacts of the sample preparation method in the latter technique, which involves drying of the sample. The sizes of the vesicles as seen in the micrographs are larger than that obtained by DLS measurement. This may be due to the fact that the latter method used filtered samples and it gives an average R_h value of broad size distribution.

3.7. ^1H NMR and FTIR spectra

The size of a molecular self-assembly is normally determined by the ionic repulsions among the surfactant head groups. The reduction of ionic repulsion causes enlargement of the size as well as packing of the hydrocarbon chains in the aggregates. When the experimental results of DMEB are compared with those of DTAB surfactant it becomes clear that formation of large vesicles by DMEB molecules is due to the aromatic moiety at the surfactant headgroup, which reduces the ionic repulsion to expand the structure. In fact, the growth of cetyltrimethylammonium bromide surfactant to produce rodlike micelles upon addition of aromatic counter ions such as tosylate, benzene sulfonate, and salicylate has been reported in the literature [55–57]. Hassan et al. [58] reported vesicle formation from cetyltrymethylammonium hydroxynaphthalene carboxylate in aqueous solution. On the other hand, Engbert and co-workers [59] have shown vesicle formation from decyltrimethylammonium–MO and dodecyltrimethylammonium–MO (MO = methyl orange) surfactants in water. It has been argued that the bulky aromatic counterions increase the hydrophobic vol-

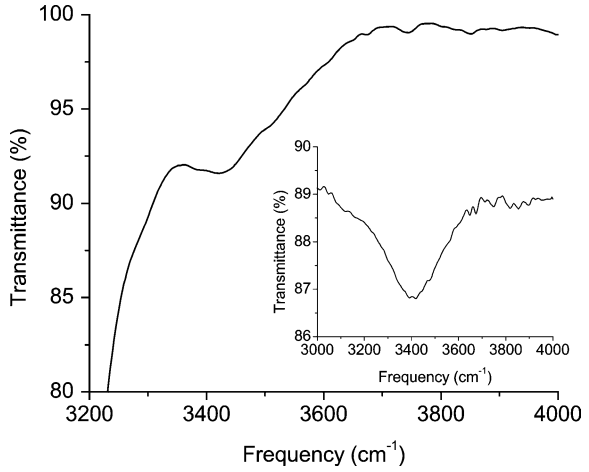

Fig. 7. FTIR spectra of solid DMEB. Inset: 8 mM solution of DMEB in D_2O.

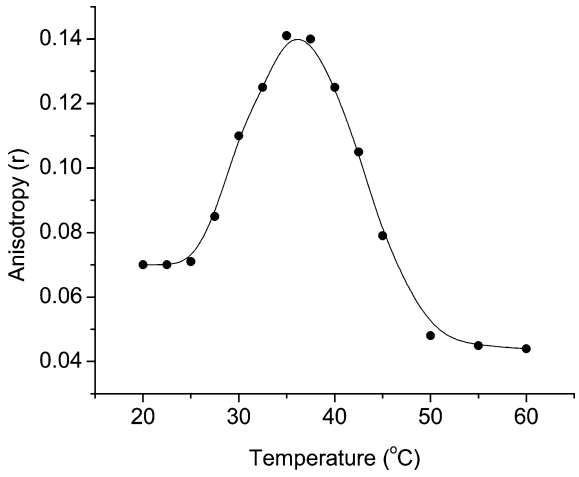

Fig. 8. Plot of fluorescence anisotropy (r) of DPH versus temperature.

ume (V) and reduce the mean cross-sectional surface area (A_0) of surfactant headgroup, thereby increasing the packing parameter, P ($P = V/A_0 l_c$, where l_c is the length of the hydrocarbon chain) [60], which usually determines the type of aggregate formed by a surfactant molecule. Accordingly, the phenyl moiety of the headgroup of DMEB surfactant must insert itself between two neighboring molecules. The presence of stereogenic centers force the phenylalkyl group of the amphiphile fold back into the aggregate interface. This is indicated by the low micropolarity and high microviscosity values (Table 1) discussed above. In order to shed light on the role of the phenyl moiety at the surfactant head group, we have recorded the ^{1}H NMR and FTIR spectra of DMEB. The ^{1}H NMR spectrum measured in D_2O above cac shows broadening of the peaks of aromatic protons compared to that in CD_3OD solvent (see Figs. 1 and 2 in the Supplementary material). This indicates that the aromatic moiety finds itself located in an environment within the aggregate where its motion is partially restricted. This results in a broadening of the NMR signals of the aromatic protons. The –OH groups of the phenylalkyl moieties of two neighboring surfactant molecules are also expected to form intermolecular hydrogen bond between two adjacent surfactant molecules. The FTIR spectrum (Fig. 7) of DMEB showed a broad band at ∼3400 cm^{-1} in the solid state, which suggests hydrogen-bonding interaction between two neighboring molecules. A similar broad band in the FTIR spectrum (inset of Fig. 7) of the molecule measured in D_2O containing 8 mM DMEB. Therefore, it can be concluded that the –OH group of the phenyl moiety is involved in hydrogen-bonding interaction with the adjacent neighbor in the aggregate. The bilayer structure formation is perhaps associated with the intermolecular hydrogen bond formation, which is facilitated at temperatures above T_K. This is supported by the variation of fluorescence anisotropy as a function of temperature as discussed below.

3.8. Phase-transition temperature

It is well known that the temperature dependence of the fluorescence anisotropy (r) of DPH can reveal phase transitions of membranes. To determine the phase transition temperature we have studied the temperature effect on r-value of DPH in 8 mM surfactant solution in the temperature range 20–60 °C. Because of the poor aqueous solubility of DMEB anisotropy value below 25 °C was measured using 5 mM solution. The plot of the variation of r as a function of temperature is depicted in Fig. 8. The anisotropy value first increases with the rise in temperature and then falls down passing through a maximum at ∼36.0 °C. The smooth rise of the r value in the temperature range 20–36 °C could be fit to a sigmoid curve corresponding to a two-state process and therefore, as already mentioned earlier, can be attributed to the transformation of micelles to vesicles in which the hydrocarbon tails of the surfactant molecules are tightly packed. This is consistent with the decrease of A_0 value upon increase of temperature. The temperature (28 °C) corresponding to the inflection point may thus be taken as the micelle-to-vesicle phase transition temperature, T_c. Interestingly, this is same as the breakpoint temperatures observed in plots of Figs. 1 and 2. This suggests that the micelle and vesicle structures are in equilibrium. The vesicle and micelle formation are respectively favored above and below T_c. Since the r-value approaches the value corresponding to bulk water, the fall of anisotropy at higher temperatures can be associated with the denaturation of vesicles. The inflection point gives the melting temperature, T_m (43.5 °C). The relatively high T_m value suggests that the vesicles are quite stable. Similar values of melting temperature have been also reported for various cationic lipids [61]. The higher melting temperature may be associated with the intermolecular hydrogen-bonding interactions among the surfactant molecules in the self-assembly that stabilizes the bilayer membrane structure. The rise of temperature (in the range 20–36 °C) enhances the rate of molecular collision and thereby facilitates formation

of intermolecular hydrogen bond between two neighboring surfactant molecules. However, at higher temperatures (>36 °C), the hydrogen bonding, as well as π–π interactions, loosens, thus making the vesicle unstable.

4. Conclusion

In summary, we have introduced a new single-tailed chiral cationic surfactant, (1R,2S)-(–)-*N*-dodecyl-*N*-methylephedrinium bromide, DMEB, which in spite of having a relatively short hydrocarbon chain self-assembles in water to form giant multilamellar vesicles above a critical temperature, T_c (28 °C). To our knowledge, in the family of dodecyltrialkyl-ammonium bromide surfactants, this is the first example that spontaneously forms giant vesicles. However, below 28 °C, the surfactant forms small micellar aggregates in water. The amphiphile has cac much less than that of DTAB surfactant. The mean aggregation number of DMEB micelles is also higher than that of DTAB. The microenvironment of the self-assemblies of DMEB is less polar and almost three times more viscous than that of DTAB micelles. The phenylalkyl moiety of the surfactant headgroup, which inserts itself between two surfactant molecules through intermolecular hydrogen bonding and π–π interactions, facilitates formation of bilayer vesicles. The TEM pictures suggest that giant vesicles are formed through fusion of smaller vesicles. The vesicles are stable within a narrow temperature range of 28–43 °C and could be observed even after 2 weeks. The stability of the vesicles at body temperature makes them suitable for uses as drug delivery vehicles.

Acknowledgments

The financial support for this work came from the CSIR (Grant 01(1664)/00/EMR-II) and DST (Grant SP/S1/G-36/99), New Delhi. S.R. thanks the CSIR for a research fellowship. The authors are thankful to Professor P. Ramamurthy and K.I. Priyadarshini for helping with the fluorescence lifetime measurements at NCUFP, Chennai. The authors also warmly thank Dr. B. Mishra, Department of Geology and Geophysics, for his help with the light microscopic measurements.

Supplementary material

The ^{1}H NMR spectra of DMEB surfactant in CD_3OD and D_2O solvents are given as supplementary material. Supplementary data associated with this article can be found on Science Direct, in the online version.

Please visit DOI: 10.1016/j.jcis.2005.05.054.

References

[1] J.H. Fendler, Membrane Mimetic Chemistry, Wiley, New York, 1982, ch. 6.
[2] T. Kunitake, in: K.L. Mittal, P. Bothorel (Eds.), Surfactants in Solution, vol. 5, Plenum, New York, 1986, p. 727.
[3] D.D. Lasic, Y. Barenholz (Eds.), Handbook of Nonmedical Applications of Liposomes, vol. 4, CRC Press, New York, 1996.
[4] D.D. Lasic, Liposomes in Gene Delivery, CRC Press, New York, 1997.
[5] A. Meager (Ed.), Gene Therapy Technologies, Applications, and Regulations, Wiley, New York, 1999.
[6] D. Needham, D.D. Lasic, Chem. Rev. 95 (1995) 2601.
[7] J.S. Martinez, G. Zhang, P. Holt, H.-T. Jung, C.J. Carrano, M.G. Haygood, A. Butler, Science 287 (2000) 1245.
[8] B.Z. Putlitz, S. Förster, K. Landfester, M. Antonietti, Langmuir 16 (2000) 3003.
[9] A.P.H. Schenning, B. De Bruin, M.C. Feiters, R.J.M. Nolte, Angew. Chem. Int. Ed. Engl. 33 (1994) 1662.
[10] K. Hanabusa, M. Yamada, M. Kimura, H. Shirai, Angew. Chem. Int. Ed. 35 (1996) 1949.
[11] P. Terech, R.G. Weiss, Chem. Rev. 97 (1997) 3133.
[12] R. Oda, I. Huc, S. Candau, Angew. Chem. Int. Ed. 37 (1998) 2689.
[13] K. Takakura, T. Toyota, T. Sugawara, J. Am. Chem. Soc. 125 (2003) 8134.
[14] H. Sakai, A. Matsumura, S. Yokoyama, T. Saji, M. Abe, J. Phys. Chem. B 103 (1999) 10737.
[15] R.T. Buwalda, J.M. Jonker, J.B.F.N. Engberts, Langmuir 15 (1999) 1083.
[16] M. Blanzat, S. Massip, V. Spéziale, E. Perez, I. Rico-Lattes, Langmuir 17 (2001) 3512.
[17] Y. Yan, J. Huang, Z. Li, F. Han, J. Ma, Langmuir 19 (2003) 972.
[18] P. Bandopadhyay, P.K. Bharadwaj, Langmuir 14 (1998) 7537.
[19] J.-H. Fuhrhop, H.H. David, J. Mathieu, U. Liman, H.-J. Winter, E. Boekema, J. Am. Chem. Soc. 108 (1986) 1785.
[20] F. Han, X. He, J. Huang, Z. Li, Y. Wang, H. Fu, J. Phys. Chem. B 108 (2004) 5256.
[21] X. Luo, S. Wu, Y. Liang, Chem. Commun. (2002) 492.
[22] O. Trager, S. Swade, C. Bottcher, J.-H. Fuhrhop, J. Am. Chem. Soc. 119 (1997) 9120.
[23] H. Hoffmann, G. Ebert, Angew. Chem. 100 (1988) 933.
[24] A. Khan, E.F. Marques, Curr. Opin. Colloid Interface Sci. 4 (2000) 402.
[25] S. Colonna, A. Re, H. Wynberg, J. Chem. Soc. Perkin Trans. 1 (1981) 547.
[26] J. Dey, A. Mohanty, S. Roy, D. Khatua, J. Chromatogr. A 1048 (2004) 127.
[27] J. Oremusová, O. Greksakova, Tenside Surfact. Deterg. 40 (2003) 90.
[28] Y. Moroi, R. Matuura, Bull. Chem. Soc. Jpn. 61 (1988) 333.
[29] S.P. Moulik, M.E. Haque, P.K. Jana, A.R. Das, J. Phys. Chem. 100 (1996) 701.
[30] K. Mukherjee, D.C. Mukherjee, S.P. Moulik, Langmuir 9 (1993) 1727.
[31] K. Mukherjee, D.C. Mukherjee, S.P. Moulik, J. Phys. Chem. 98 (1994) 4713.
[32] Y.-Y. Won, A.K. Brannan, H.T. Davis, F.S. Bates, J. Phys. Chem. B 106 (2002) 3354.
[33] R. Zana, in: R. Zana (Ed.), Surfactant Solutions: New Methods of Investigation, Dekker, New York, 1987, ch. 5.
[34] K. Kalyansundaram, Photophysics of Microheterogeneous Systems, Academic Press, New York, 1988.
[35] J.K. Thomas, The Chemistry of Excitation at Interfaces, in: ACS Monographs, vol. 181, Am. Chem. Soc., Washington, DC, 1984.
[36] F.M. Winnik, S.T.A. Regismond, Colloids Surf. A 118 (1996) 1.
[37] D.C. Dong, M.A. Winnik, Photochem. Photobiol. 35 (1982) 17.
[38] K. Kalyanasundaram, J.K. Thomas, J. Am. Chem. Soc. 99 (1977) 2039.

[39] U. Cogan, M. Shinitzky, G. Weber, T. Nishida, Biochemistry 12 (1973) 521.
[40] M. Shinitzky, Y. Barenholz, J. Biol. Chem. 249 (1974) 2652.
[41] K.A. Zachariasse, W. Kuenle, A. Weller, Chem. Phys. Lett. 73 (1980) 6.
[42] R. Zana, M. In, H. Lévy, Langmuir 13 (1997) 5552.
[43] M. Shinitzky, I. Yuli, Chem. Phys. Lipids 30 (1982) 261.
[44] M. Shinitzky, in: Physical Methods on Biological Membranes and Their Model Systems, Plenum, New York, 1984, p. 237.
[45] J.T. Edward, J. Chem. Ed. 47 (1970) 261.
[46] M. Shinitzky, A.-C. Dianoux, C. Itler, G. Weber, Biochemistry 10 (1971) 2106.
[47] G.B. Dutt, J. Phys. Chem. B 108 (2004) 3651.
[48] M. Tachiya, Chem. Phys. Lett. 33 (1975) 289.
[49] N.J. Turro, A. Yekta, J. Am. Chem. Soc. 100 (1978) 5951.
[50] S.D. Wettig, P. Nowak, R.E. Verral, Langmuir 18 (2002) 5354.
[51] P.C. Heimenz, Principles of Colloid and Surface Chemistry, second ed., Dekker, New York, 1986.
[52] P.A. Hassan, S.R. Raghavan, E.W. Kaler, Langmuir 18 (2002) 2543.
[53] F.E. Antunes, E.F. Marques, R. Gomes, K. Thuresson, B. Lindman, M.G. Miguel, Langmuir 20 (2004) 4647.
[54] M. Mu, F. Ning, M. Jiang, D. Chen, Langmuir 19 (2003) 9994.
[55] V.K. Aswal, J. Phys. Chem. B 107 (2003) 13323.
[56] T. Shikata, H. Hirata, T. Kotaka, Langmuir 4 (1988) 354.
[57] C. Gamboa, L. Sepúlveda, J. Colloid Interface Sci. 113 (1986) 566.
[58] P.A. Hassan, J. Narayanan, S.V.G. Menon, R.A. Salkar, S.D. Samant, C. Manohar, Colloids Surf. A 117 (1996) 89.
[59] R.T. Buwalda, J.M. Jonker, J.B.F.N. Engberts, Langmuir 15 (1999) 1083.
[60] J.N. Israelachvili, J.J. Mitchel, B.W. Ninham, J. Chem. Soc. Faraday Trans. 2 72 (1976) 1525.
[61] S. Bhattacharya, P.V. Dileep, J. Phys. Chem. B 107 (2003) 3719.